SMART CONTROL OF SEPARATION AROUND A WING
- control system -

Akira NISHIZAWA and Shohei TAKAGI
Japan Aerospace Exploration Agency, Chofu, Tokyo, 182-8522

Hiroyuki ABE, Takehiko SEGAWA, and Hiro YOSHIDA
National Institute of Advanced Industrial Science & Technology, Namiki, Tsukuba, 305-8564

Abstract

This paper demonstrates a new smart control system to suppress flow separation around a wing model, which comprises a separation discriminator, an intelligent controller and a row of disturbance generators. As soon as the discriminator detects a harbinger of separation, the controller with separation control algorithm activates the generators, which simultaneously inject periodic disturbances from the leading edge. It is shown that the smart control system managed by a computer effectively delays the occurrence of stall.

1. Introduction

Numerous researches made on separation control[1)] had provided much advanced understandings on mechanism of control. Nowadays primary aims of these researches have moved on to development and integration of practical devices such as actuators[2)] and sensors[3)], and utilization of algorithm[4)]. Our goal in the MEMS subgroup is establishment of a smart wing system with the automatic separation control and detection. NASA[5-6)] and many others have created high lift device by applying ideas of flow control to improve airplane performance in landing and take-off regimes. For such goal, open-loop control is sufficient and flow separation detection is not an important issue. Upon scheduled flight, timing of separation control is predetermined. In prospect that future small aircraft has much higher degree of freedom in flight mission and other new types of air vehicles such as unmanned aerial vehicles have come to be in the limelight as application objective using flow control, our target application places on the smart wing with closed-loop control system. The role of our smart wing is avoidance from dangerous stall due to unexpected environmental causes, human errors, failures and so on, rather than improvements of maximum lift. As stated by McCormick et at[7)], packaging of a self-contained actuator inside the confined leading edge of the airfoil represented a significant challenge. Establishing a compact control system to be installed in a small wing seems to be more important.

So far, this subgroup has investigated the devices such as micro jet vortex generator (MJVG), piston type actuator, and reverse flow sensor. Takagi et al. [8)] and Nishizawa et al. [9)] used a new MEMS sensor as a reverse flow detector in a simple separated flow on an inclined plate. The MEMS sensor has been originally developed by Ozaki et al.[10)] for a model of wind receptor hairs of insects. Nishizawa et al.[11)] examined performance of the MEMS sensor in a flow around a wing model and demonstrated the utilization of the sensor. The present study aims to verify the effect of the control system with integration of all devices[9,11,12)] previously developed into a wing model and to establish a smart wing model with feedback control algorithm.

2. Experimental Apparatus

2.1 Wind tunnel and wing model

A NACA0015 wing model was used in the present experiment since its trailing edge stall characteristic was useful to estimate the arrangement of actuators and a separation sensor. The wing model was placed at the center of the test section of a suction-type wind tunnel. The maximum flow speed is 18 m/s. The turbulence intensity of the free stream is less than 0.3% at a free stream velocity of 10m/s. A schematic view of the test section is shown in Fig.1. The size of test section is 1500mm in length, 600mm in height, 300mm in width. Its chord length, c, is 200mm, spanwise length, b, is 300mm and aspect ratio, b/c, is 1.5. The angle of attack, α, is set by a rotary table. The free-stream velocity, U_∞, is defined as the velocity where the Pitot tube is located. The experiments were conducted at U_∞=10m/s. The Reynolds number, R_e, based on the chord length and U_∞ is nominally 1.4×10^5. Uncertainty of the Reynolds number due to ambient temperature drift is kept within ±8%. In the coordinate system, x and z' are the chord wise and vertical direction respectively.

Figure 2 shows the picture of the smart wing model. Six small actuators developed at AIST[12] were installed near the leading edge. Twelve 0.5 mm diameter holes were drilled at the leading edge (x/c=0) in the spanwise direction. Input lines of these actuators are connected in series.

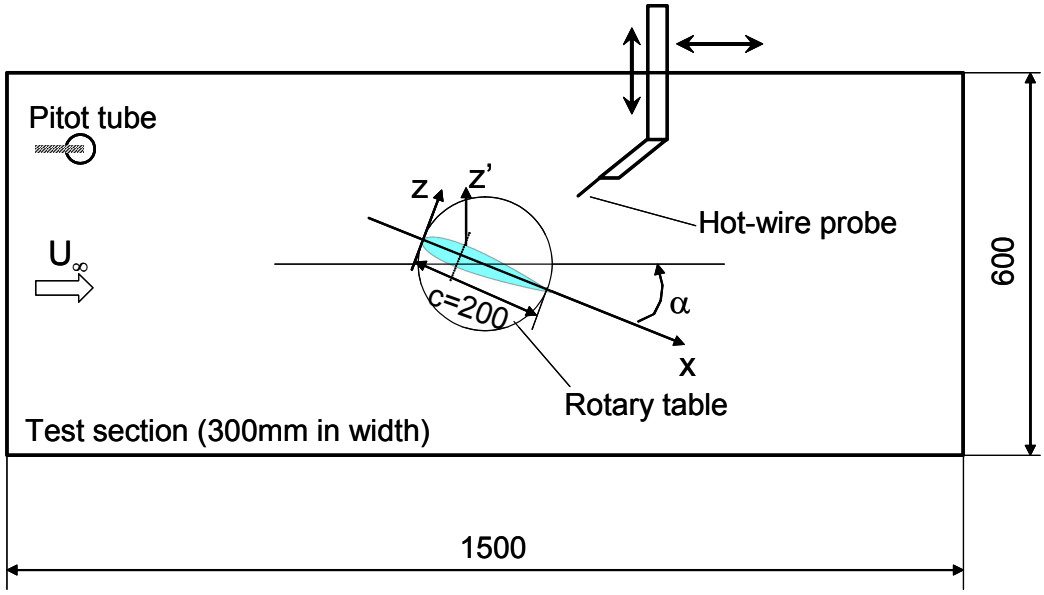

Fig.1 Experimental setup (unit:mm).

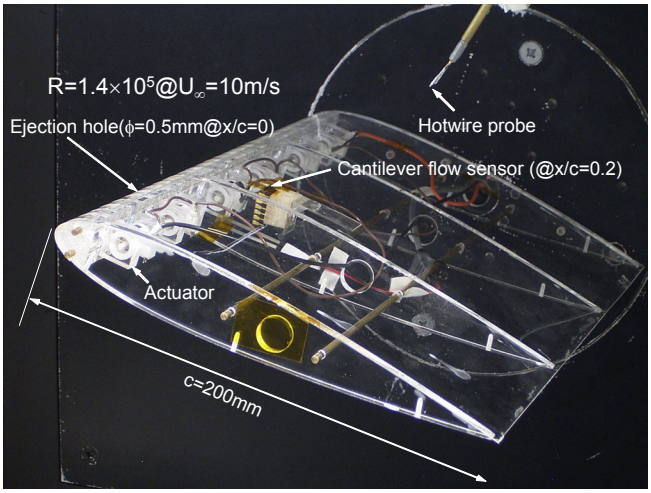

Fig.2 NACA0015 wing model

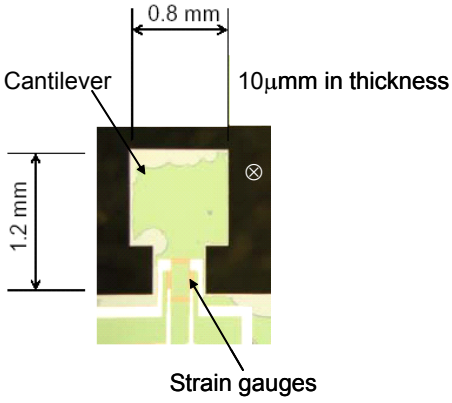

Fig.3 Cantilever flow sensor.

2.2 Separation detector

A cantilever flow sensor (CFS) as shown in Fig.3, was used as a reverse-flow detector. The CFS was installed at x/c=0.2 off the centerline. This sensor was produced using MEMS Technology and consisted of a cantilever and strain gauges. The cantilever is 0.8 mm in width and 0.01mm in thickness. It has strain gauges at the root near the base to interpret flow direction: the sensor output for reverse flow indicates the negative sign, and vice versa. The original idea for the sensor was proposed and verified[10] by professor Simoyama's group in Tokyo University and our group fabricated the improved configuration. Although the sensitivity for separated boundary layers was verified in our previous papers[9,11], the problem of temperature sensitivity about this type of sensor was also suggested through these studies. To reduce the thermal drift, the sensor was placed so that its strain gauges avoided of being exposed to the flow. The ambient temperature in the flow was simultaneously recorded with the sensor output and the drift level was estimated through the measurements. This manner, however, cannot completely delete the error due to thermal drift. Since a compensation technique based on the correlation between the ambient temperature and the sensor output is under examination in our group now, such technique can be established in the near future wing model experiments.

2.3 Actuator

We developed two types of actuators as shown in our previous papers. One is micro jet vortex generator (MJVG)[12] with steady blowing and another is small piston type actuator [12] with periodic blowing and suction. In the present study, the piston type actuators were chosen since its unsteady characteristic was more suitable for the validation of the feedback control system.

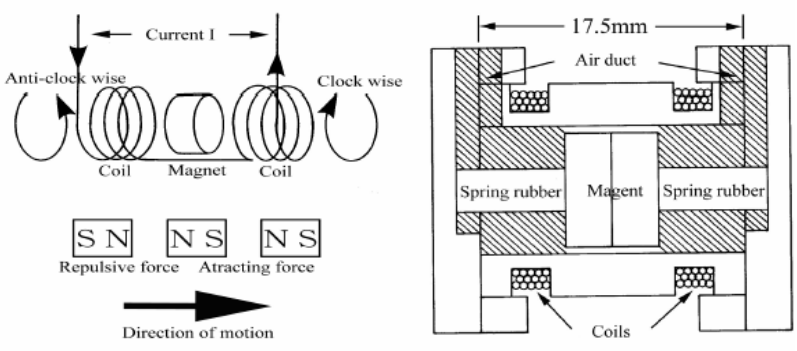

Fig.4 Small piston type actuator.

Definite evidence that excitation of a boundary layer by periodic disturbance can delay separation was shown in the detailed investigations by Seifert et al[13]. As mentioned below, the blowing momentum of our piston-type actuators is about 100 times less than that of Seifert et al[13]. They used an external small centrifugal blower with rotary valve to introduce the periodic blowing unlike our internal actuators. Although such internal actuator has disadvantage of poor momentum, it provides an indispensable advantage of a built-in device for a smart wing. Figure 4 shows the driving principles and geometry of the actuator. Cylindrical spring rubbers in the both sides connect the magnet. Windings directions of the coils in the both sides of the magnet are opposite so as to generate forces, which tend to bring the magnet towards the neutral position. Figure 5 shows an example of time trace of the hot-wire output measured above the leading-edge hole for no wind at disturbance frequency of f=20Hz. The trace indicates that the strong blowing and weak suction repeated at the period of the actuator oscillation. Since the hotwire cannot detect the flow direction, blowing and suction phases are assumed. The magnitude of the disturbance, V_j', is defined by the root mean square of the fluctuating velocity. Figure 6 shows the magnitude of V_j' against avtuator input voltage for various frequency. Unlike conventional loud speakers or synthetic jet[2], the actuator is more efficient in the very low frequency range such as 5 - 40 Hz as shown in this figure, corresponding to the dimensionless frequency $F^+=fc/U_\infty$ of 0.1-0.8 under the present experimental condition. These values are within the frequency range that Seifert et al[13] observed the effect on

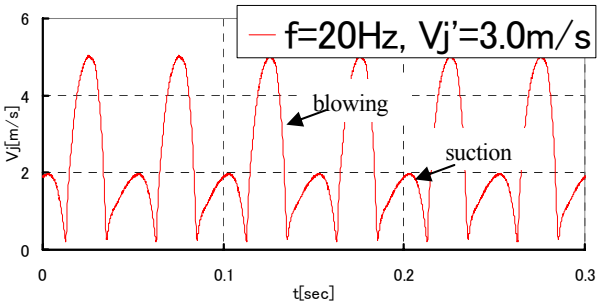

Fig.5 Time trace of the hot-wire output, V_j, measured above the ejection hole (z'=0.5mm) for no wind at f=20Hz.

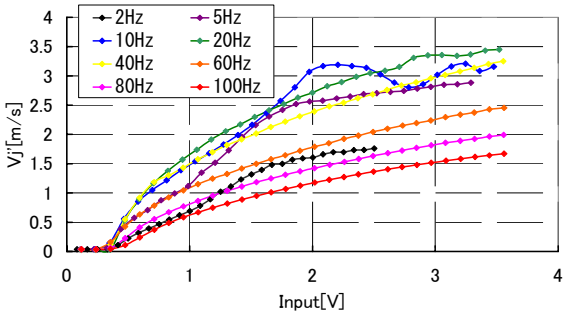

Fig.6 Relation between actuator input and output for various frequencies.

the lift increasing.

2.4 Control System and data acquisition

In the previous papers[9,11], we examined the very simple on-off control algorithm with a constant magnitude of the disturbance for the wing model. The role of separation detector was only "switch" at that system. In the present paper, the control algorithm was modified by means of the feedback loop. The schematic view of feedback control system is shown in Fig.7. The CFS output is acquired by a computer through an A/D converter and the output signal is processed into the input signal to the actuators. The durations for acquisition and operation of actuators in a loop can be adjusted.

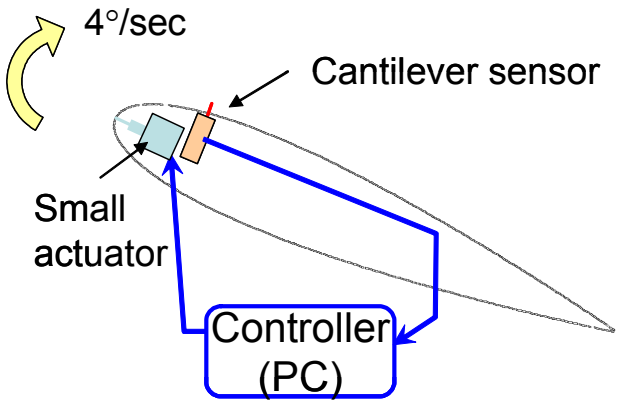

Fig.7 Schematic view of the feedback control system.

The velocity in flow around the wing was measured by a conventional constant-temperature hot-wire anemometer and a single-wire probe. The lift coefficient, C_L, is directly measured by force sensor installed in the rotary table. The uncertainty of C_L is kept within $\Delta C_L = \pm 0.05$. The ambient temperature is measured by means of thermocouple. The outputs from the anemometer, force sensor, thermocouple and separation detector were acquired by 16 bit A/D board installed in the computer.

3. Result and discussion

3.1 Open-loop control by periodic disturbances

Figure 8 shows C_L distributions for variation of the disturbance magnitude at constant frequency of 20 Hz. Larger magnitude of the disturbance brings better effect on the lift recovery. Since the actuator output came up to almost the limitation level for V_j' =3.0m/s, we could not confirm the optimum value in the V_j'. Figure 9 shows the effect of disturbance frequency on the C_L distributions at the constant disturbance magnitude. The result shows that the lift recovery effect depends on the frequency. In our previous paper[11], we concluded that the lift recovery effect was independent of the disturbance frequency. The difference in frequency range tested seems to contribute to the difference between the previous and present results. The frequency range was 50 – 1000 Hz for the previous experiment since the small loud speakers were used as actuators, in contrast with 2 – 100 Hz for the present experiment. Lower and higher limits of the effective frequency are as important as the optimum frequency because such limits are related to the design requirements for development of new actuators.

Effects of the magnitude and frequency of the disturbances on the lift recovery are summarized and compared with the results by Seifert et al.[13] in Fig.10. The disturbance magnitude is normalized by the equation as $\langle c_\mu \rangle = 2(H/c)\cdot(V_j'/U_\infty)^2$ where, H is height of the blowing slot at the leading edge for the experiments by Seifert et al. Since the configuration of blowing spout is not two-dimensional slot but the circular holes for the present wing model, H is estimated as $H=\pi(\phi/2)^2 n/b$, where ϕ is the diameter of hole, n is the number of holes and b is the spanwise length of the model. As mentioned above, the output level of our actuators is much lower than that of the air supplier used by Seifert et al. In spite of such disadvantage, the actuator has certain effect on the increasing of lift, although the maximum increment in the present results is much lower than that of optimal value of $\langle c_\mu \rangle \approx 0.05$ for Seifert et al. This result encourages us, because even very low-consumed actuators can effectively prevent stall for actual airplanes such as small unmanned air vehicle or low-cost manned small plane. Toward practical applications, we need more investigations about Reynolds number dependency, optimal arrangement of the blowing holes, mechanical durability of the actuators and so on.

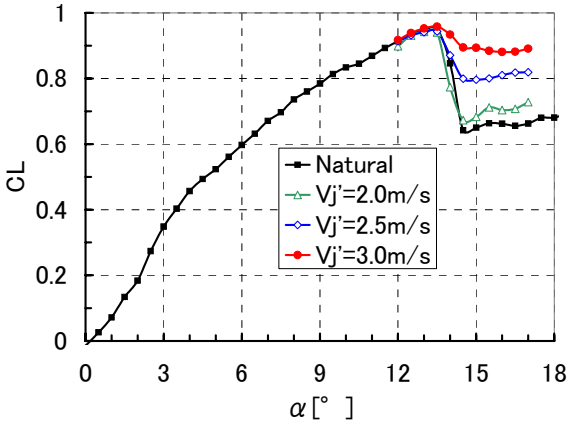

Fig.8 C_L distributions for various angles of attack and disturbance magnitude at f=20Hz.

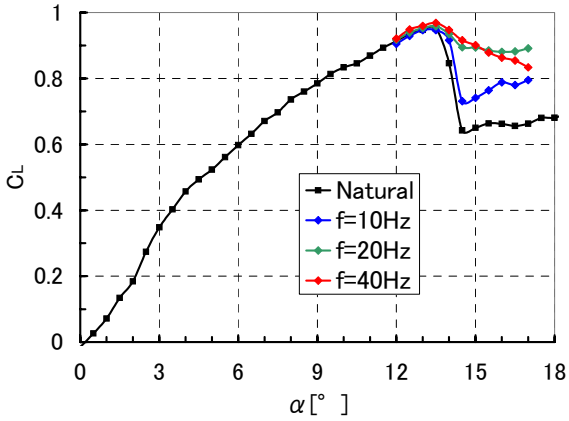

Fig.9 C_L distributions for various frequencies at constant disturbance magnitude of V_j'=3.0m/s.

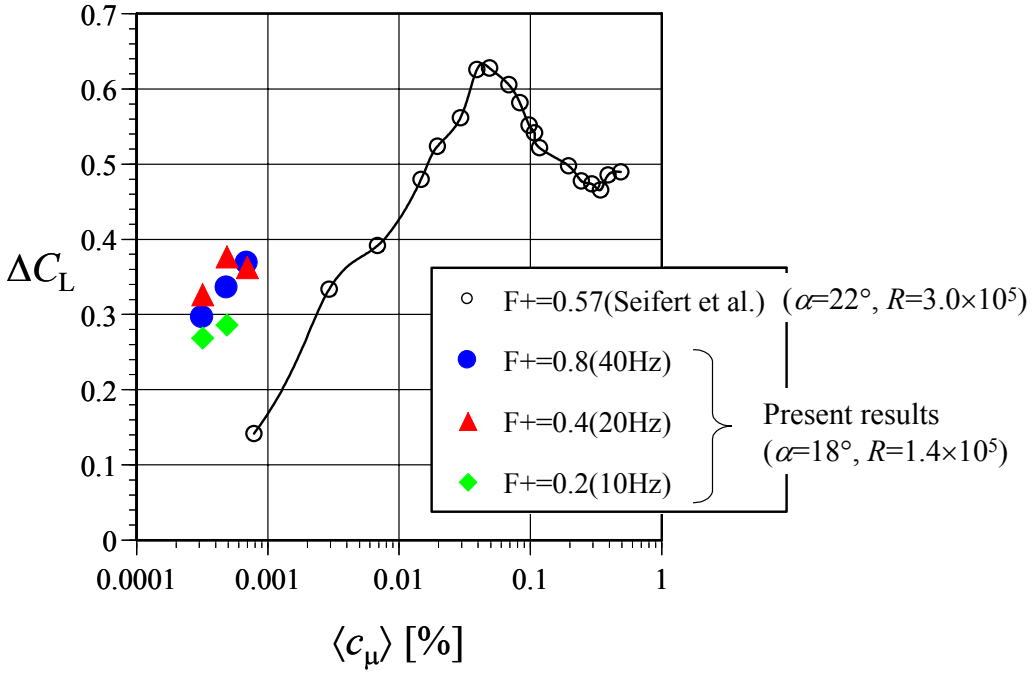

Fig.10 Effects of disturbance magnitude, $\langle c_\mu \rangle$, on increasing of the lift coefficient, ΔC_L.
Note that Seifert et al[13] measured at α=22° in contrast with the present experiments at α=18°. In our experiments, uncertainty in the C_L measurements became much larger for α>20°due to the low aspect ratio of the wing model.

Figure 11 shows the variation of the time averaged DC and AC components of the CFS output for the various angles of attack. As shown in Fig.11a, the DC component, abruptly varies from positive to negative when the angle of attack exceeds the stall angle of α=13.5° for the natural case without any control. The behavior of the CFS output for the occurrence of flow separation on the wing indicates the utility of CFS as a separation detector. For the case with control, however, the DC output does not become positive above the stall angle in spite of the apparent lift recovery as shown in Fig.8. The reason why the averaged CFS output does not come to plus is indicated in Fig.12. The figure shows the time traces of instantaneous output of CFS and actuator driving pulse at constant angle of α=18°. The instantaneous waveform indicates that the forward flow only intermittently appears at relatively low frequency even in the controlled state. As shown in the instantaneous waveform, the behavior of flow around the wing seems to be cyclically switching between two flow states as separated and attached. Therefore, the aspects in AC component of the CFS output are different

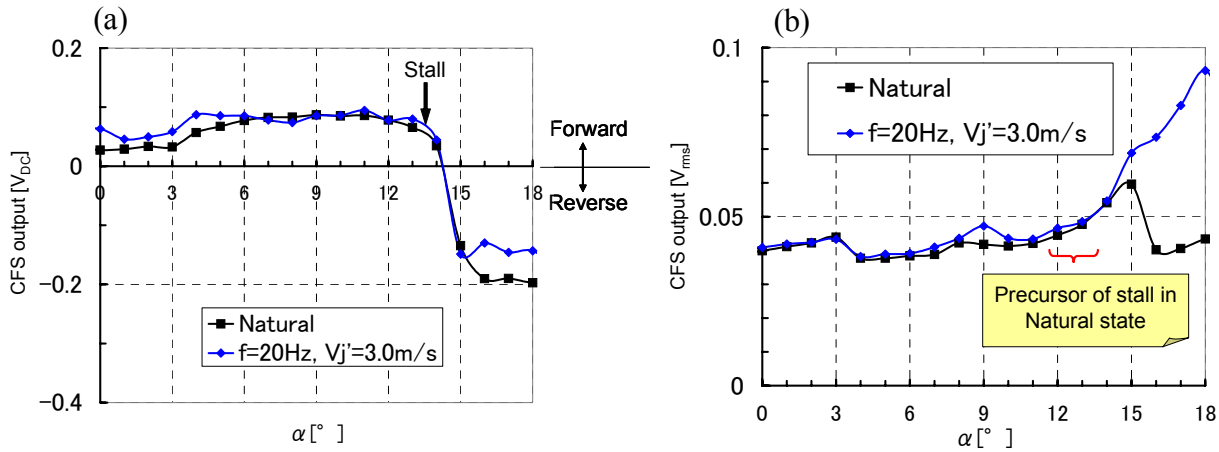

Fig.11 Distributions of time averaged cantilever flow sensor output for various angles of attack. (a)DC component, (b)AC component.

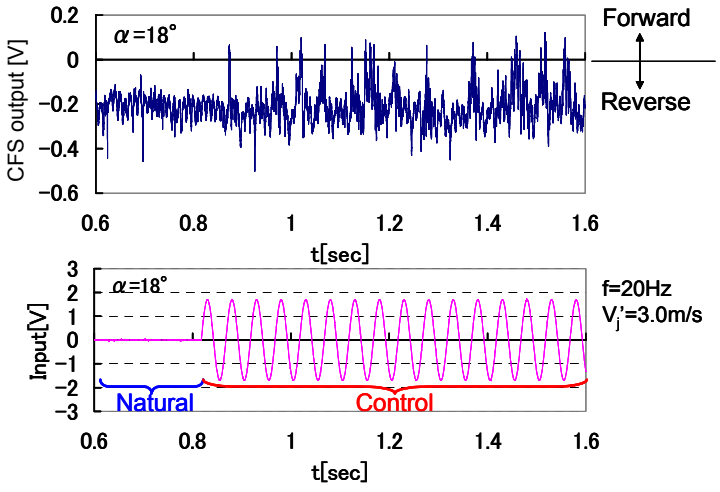

Fig.12 Instantaneous waveforms of CFS output and actuator driving pulse at α=18° and x/c=0.2.

from that of the DC component as shown in Fig.11b. It is worthwhile noting that the AC component of the CFS output gradually increases at α=12° just before stall, while the DC output tends to simply decrease. This increase of AC component indicates the precursor of stall.

3.3 Establishment of the feedback control system

As the CFS response to the flow separation was confirmed, the output of the CFS was examined to feed into the actuators. The proportional feedback algorithm can be described by the simple equation as

Input=$A\sin ft$ (A=0 if CFS output >0, A∝CFS output if CFS output <0)

where A is the amplitude of actuator driving pulse. In this system, the frequency was fixed at f=20Hz based on the results in open-loop control. The similar feedback algorithm was already used by the recent paper by Glauser et al [4] for the separated flows on a wing model. They used multiple surface pressure sensors as the detection sensor of flow separation in combination with Proper Orthogonal Decomposition analysis. Our method has an advantage that the flow separation can be directly discriminated without any complex analyses. Such advantage allows us to minimize the time lag due to processing through the A/D hardware and computer. To demonstrate the feedback control system it was operated when the angle of attack was continuously increased by the rotary table at constant speed of about 2°/s. Figure 13 shows the time traces of CFS output signal and actuator driving pulse in both cases with and without control. In case of the natural state, the CFS output decreases with the increased angles of attack and the reverse flow appears around the stall angle. When the control system is operated, the actuator driving pulse gradually amplifies with decreased CFS output and then the forward flow signal intermittently appears even after the occurrence of the stall, indicating that the automatic detection and feedback control system works well.

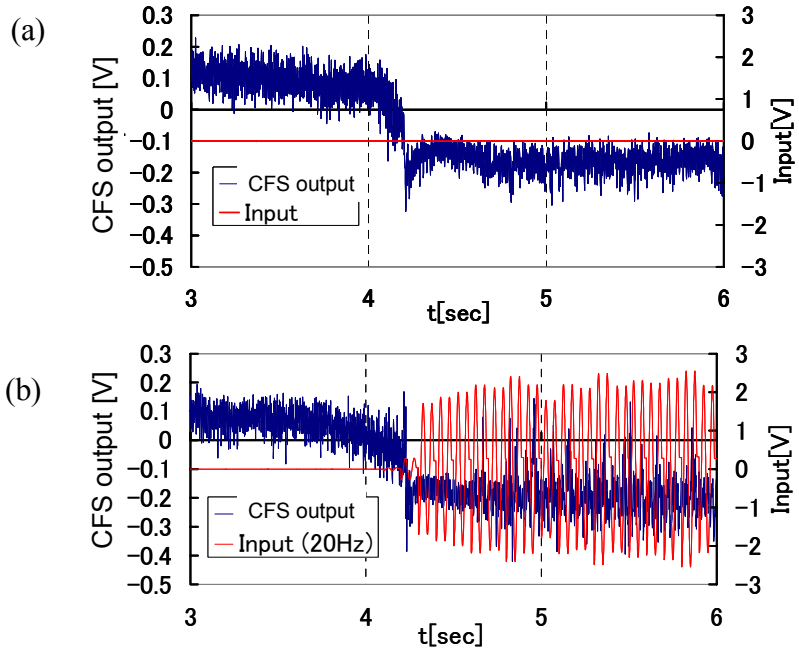

Fig.13 Demonstration of the control system for the pitching motion of the wing. (a) CFS output without control, (b) CFS output and actuator driving pulse with control.

4. Concluding remarks and proposal toward practical applications

In the present study, the active separation control system was applied to a wing model. The utility and possibility of the built-in actuators were confirmed for the flow separation on the wing. The discriminator made use of MEMS technology worked well as a stall-warning device. The system integration was established for the wing model and the smart control system with feedback loop was demonstrated for the pitching motion of the wing.

Although the components and algorithm in the present system are very simple, the MEMS sensor is very brittle. The new surface mountable sensors based on optical method developing in AIST to improve the robustness of the control system are anticipated to replace the current sensor. For the actuators, more investigations are needed about Reynolds number dependency, optimal arrangement of the blowing holes, mechanical durability and so on toward the practical applications.

Acknowledgements

The authors would like to thank T. Kojima, T. Takahashi and Y. Hashimoto for helping built the data acquisition system.

References

1) Gad-el-Hak, M., 2000, *Flow control*, Cambridge Univ. Press.
2) Glezer, A. and Amitay, M., "Synthetic Jets", 2002, Annu. Rev. Fluid Mech. Vol.34, pp.503-529.
3) Jiang, F., Tai, Y. C., Walsh, K., Tsao, T., Lee, G.B. and Ho, C. M., 1997 , "A Flexible MEMS Technology and Its First Application to Shear Stress Sensor Skin", *IEEE MEMS-97 Workshop Japan*.
4) Glauser, M. N., Higuchi, H., Ausseur, J. and Pinier, J., 2004, "Feedback Control of Separated Flows", *2nd AIAA Flow Control Conference*, *AIAA* paper, 2004-2521.
5) McLean, J.D., Crouch, J.D., Stoner, R.C., Sakurai, S., Seidel, G.E., Feifel, W.M., Rush, H.M., 1999, "Study of the application of separation control by unsteady excitation to civil transport aircraft", *NASA/CR*-1999-209338, pp.1-59.
6) Anders, S. G., Sellers Ⅲ, W. L. and Washburn, A. E., 2004, "Active Flow Control Activities at NASA Langley", *2nd AIAA Flow Control Conference*, *AIAA paper*, 2004-2623.
7) McCormick, D.C., Lozyniak, S.A., MacMartin, D.G., Lorber, P.F., 2001, "Compact, high-power boundary layer separation control actuation development", *ASME paper* FEDSM2001-18279.
8) Takagi,S., Tokugawa, N., Nishizawa, A., Abe, H., Kikushima, Y., Maeda, R., Yoshida, H., 2002, "Toward smart control of separation around a wing", *Proc. 3rd Symp. Smart Control of Turbulence*, Univ. Tokyo, March 3-5, pp.9-14.
9) Nishizawa,A., Takagi,S., Abe,H., Maeda,R., Yoshida,H., 2003, "Toward smart control of separation around a wing –Development of an active separation control system-", *Proc. 4th Symp. Smart Control of Turbulence*, Univ. Tokyo, March 2-4, pp.13-21.
10) Ozaki, Y., Ohyama, T. Yasuda, T. and Shimoyama, I., 2000, "An air flow sensor modeled on wind receptor hairs of insects", in Proc. MEMS 2000, Miyazaki, Japan, Jan. 23-27.
11) Nishizawa,A., Takagi,S., Abe,H., Segawa,T., Yoshida,H., 2004, "Toward smart control of separation around a wing –Active separation control system part2-", *Proc. 5th Symp. Smart Control of Turbulence*, Univ. Tokyo, February 29- March 2, pp.7-14.
12) Abe,H., Segawa,T., Kikushima,Y., Yoshida,H., Nishizawa,A., Takagi,S., 2004, "Toward smart control of separation around a wing –Active separation control device part2-", *Proc. 5th Symp. Smart Control of Turbulence*, Univ. Tokyo, February 29- March 2, pp.15-20.
13) Seifert, A., Darabi, A., Wygnanski,I., 1996, "Delay of airfoil stall by periodic excitation", *J. Aircraft*, 33, pp.691-698.
14) Abe, H., Segawa, T., Matsunuma, T., Yoshida, H., 2001, "Micro jet vortex generator for active control of flow separation", *Proc. International Conference on Power Engineering*, Oct.8-12, 2001, Xi'an China.